3 Paragenesis

This chapter identifies the paragenetic history of Kucing Liar by documenting the small-scale controls of fluid infiltration, alteration mineralogy and the sequence of mineral development. A large number of minerals are developed during hydrothermal infiltration and some effort is taken to describe and illustrate the various forms and crosscutting relationships in each case. A significant problem at Kucing Liar results from varying wall rock composition and the alteration characteristics are defined here in terms of host rock lithology in order to recognise that influence. The procedures used to define the characteristics of the hydrothermal system are:

1. Identification of minerals generated during hydrothermal activity

2. Determination of paragenetic sequence from crosscutting relationships

A number of drill holes from the main mineralised zone were examined in detail to identify the primary mineralogy and their textures. Samples were collected from split drill core. Thin sections and polished slabs were prepared from each section. Photographs of the split drill core samples are used to illustrate the styles of mineral occurrence and their small-scale structural controls. Initial identification of minerals present in drill core samples was followed by targetted petrography to confirm the identity of many minerals. Mineral compositions are derived from quantitative element oxide analyses collected from a Jeol JXA-600 SEM-EDS microprobe (Appendix III). An XRD method termed GADDS (General Area Detection Diffraction System) was found to be very useful as it is a non-destructive technique that can be applied to mesoscopic (up to 10cm-scale) specimens mounted on a traversable stage and targetted using high magnification video (Figure 3-1, Figure 3-4). Due to the nature of the technique it was possible to analyse individual millimetre-scale alteration bands, which were difficult to distinguish in thin sections.

3.1 MINERAL TEXTURES, ASSEMBLAGES AND TIMING RELATIONSHIPS

Observations of crosscutting relationships were generally confined to examination of split and polished core samples. Minerals occur in a range of textures, including penetrative or selvedge alteration as well as vugh and fracture infill. In the following descriptions, "penetrative alteration" implies no distinct fluid channelway can be observed while selvedge alteration infers the presence of a fluid conduit. "Vein" is used when referring to planar centimetre-scale infill while "fracture infill" refers to millimetre-scale irregular features. The specific temporal relationships between minerals are generally found in crosscutting veins and in particular, their alteration selvedges. Breccia textures were also useful in confirming relationships. The dominant minerals are placed into paragenetic groups based on relative timing. The hydrothermal minerals identified are placed into four groups which reflect similar broad-scale temporal relationships built up by specific timing relationships found in disparate individual samples. Some of these groups are chemically similar while others are not. The minerals within each group generally reflect similar fluid infiltration styles based on the textural setting of mineral development.

Group I paragenesis

This group is a collection of chemically-related calc-silicate and magnesian-silicate parageneses that can be divided into early anhydrous minerals and later hydrous minerals. The inclusion of calcite-magnetite in this group is due to consistent spatial relationships of these minerals to calc-silicate alteration. The parageneses are:

a) Calcite ± magnetite — $CaCO_3$, Fe_3O_4

b) Clinopyroxene ± plagioclase — $Ca(Mg,Fe)Si_2O_6$, $(Ca,Na)(SiAl)_4O_8$

c) Grossular-andradite — $Ca_3Al_2Si_3O_{12} – Ca_3(Fe^{3+},Ti)_2Si_3O_{12}$

d) Humite ± forsterite — $Mg(OH,F)_2 \cdot 3Mg_2[SiO_4]$, Mg_2SiO_4

e) Chrysotile-serpentine — $Mg_3Si_2O_5(OH)_4$

f) Tremolite-actinolite — $Ca_2(Mg,Fe)_5Si_8O_{22}(OH)_2$

Calcite ± magnetite

The earliest hydrothermal mineral association is characterised by calcite plus locally significant amounts of magnetite. Calcite is white, grey, black or orange. It occurs in a variety of forms ranging from penetrative alteration, millimetre and centimetre-scale selvages along simple fractures to complex convoluted bands, while the associated magnetite is developed as discrete spots, commonly but not invariably associated with a recognisable fracture. Where calcite ± magnetite alteration has developed in shale it is uniformly black to dark grey in appearance and very fine-grained with no visible evidence of fluid channelways. Calcite ± magnetite is consistently crosscut by clinopyroxene ± plagioclase (Plate 3-1a, c, e).

Clinopyroxene ± plagioclase

Clinopyroxene ± plagioclase development is typically penetrative and forms relatively sharp contacts with zones of calcite ± magnetite. This alteration produces two very distinct textures depending on whether it is developed in limestone or calcareous shale (Plate 3-1c, f). Plagioclase feldspar (labradorite composition) occurs in subequal quantities with clinopyroxene in calcareous shale but is sporadic in limestone precursors. Rare examples of white plagioclase-only alteration were found (Plate 3-1d). Sedimentary textures of sandstone, limestone/dolostone and shale are generally preserved by clinopyroxene ± plagioclase alteration whose colour and appearance varies consistently with host unit. In limestone and dolostone, the colour of clinopyroxene ± plagioclase varies from white to light green, while it is persistently darker green and much finer-grained where developed in shale (Plate 3-1c). Petrographic studies reveal patterns of clinopyroxene grainsize that are coincident with the sedimentary rock texture. It is formed as evenly spaced rosettes of coarser-grains radiating from a fine-grained core in sandstone and as coarse-grained accumulations in a very fine-grained groundmass in peloidal limestone. In shale precursors, clinopyroxene grains are evenly scattered and fine to very fine-grained, and where distinguishable are yellow in contrast to their colourless appearance in limestone.

Rare examples of fluid channelways were recognised during SEM analysis where clinopyroxene is concentrated immediately adjacent to a fracture. These fractures also contained µm-scale infill. Analyses of clinopyroxene conform to a general formula of $Ca(Mg,Fe)Si_2O_6$ ranging from diopside (Hd_{05}) to hedenbergite (Hd_{60}) (Figure 3-2a). The variation of clinopyroxene composition is closely related to lithology. Those in altered limestone/dolostone are restricted to $<Hd_{20}$, whereas samples from shale have a much larger range in compositions from Hd_{20}-Hd_{60}. Clinopyroxene in porphyry host units has an intermediate composition close to Hd_{20} (Figure 3-2a). Plagioclase developed during Stage I in conjunction with clinopyroxene has two compositional groupings respectively, between An_{20} and An_{40} and closely grouped about An_{60}. Secondary plagioclase developed in porphyry is typically low in albite while in limestone it is more albitic and more varied in composition (Figure 3-2). Plagioclase developed in shale has compositions similar to porphyry and limestone-hosted plagioclase. Plagioclase accompanies clinopyroxene in calcareous shale while clinopyroxene is darker green in hornfelsed shale reflecting higher iron contents (see Chapter 1, Table 1-5).

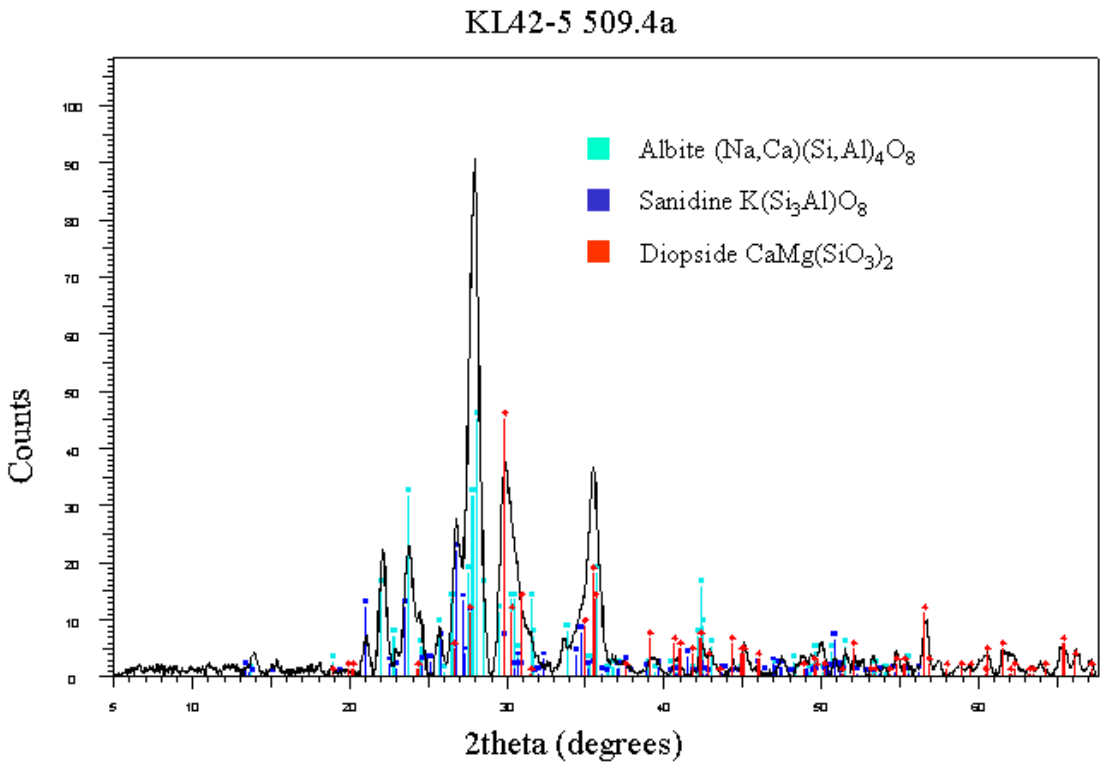

Figure 3-1 Example of GADDS X-ray diffraction identification of hornfels alteration in shale

An overlay of output from an X-ray diffraction analysis from GADDS equipment on library signatures.

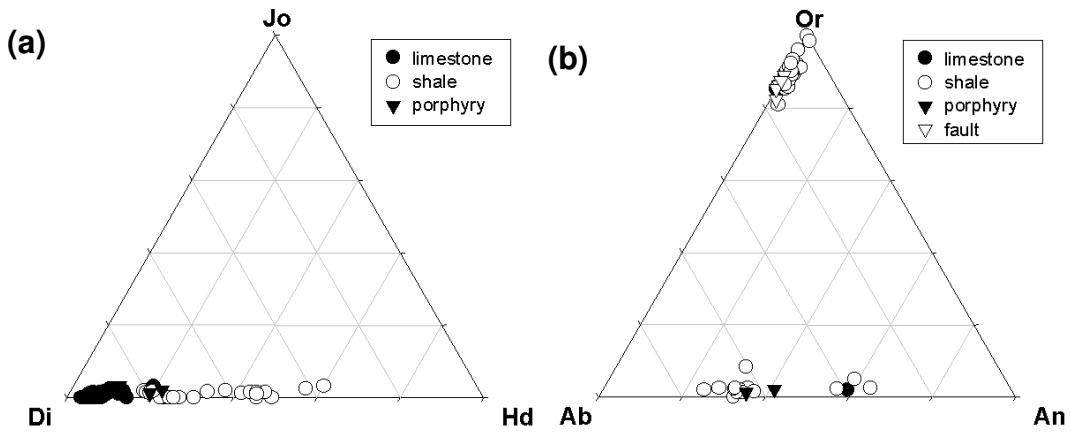

Figure 3-2 Composition of clinopyroxene and feldspar

(a) Clinopyroxene analyses show the chemical control exerted by protolith (b) Plagioclase and orthoclase feldspar compositions identify individual mineral compositions populations but no influence imposed by wall rocks.

Garnet

Garnet varies from green through red, orange and brown intermediate colours in limestone, frequently in the same hand specimen, but is consistently red where developed in shale. Garnet commonly forms 1-10cm scale accumulations that parallel identified sedimentary layering in shale, though widths of 20-50m were observed in drill core (see Chapter 4). In one instance (Plate 3-1e) garnet was observed to occupy the centre of a vein with a pale green clinopyroxene selvedge. It is difficult to discriminate between infill and alteration garnet, although examples of recognised infill garnet suggest it forms darker shades of the same colour. The petrographic character of garnet varies in that the green and red varieties are both isotropic, while brown garnets are anisotropic and display concentric growth zones. Garnet timing is problematical and it is possible that the different garnets, coloured from red to green, perhaps developed at different times (Plate 3-1g). Garnet overprints both diopside and hedenbergite ± plagioclase. There appears to be an early green garnet that was overprinted by brown to red garnet. Green garnet is crosscut by green phlogopite and also by red garnet, while red garnet crosscuts K-feldspar (Plate 3-1h).

Garnet compositions are generally consistent within a single sample (Appendix III) except for sample KL26-8 385.4, which contains two types of garnet (green and red). The primary compositional trend lies along the andradite-grossular series ranging from Ad_{100} to Ad_{40}, the spessartine, pyrope and almandine components within this trend having maxima of Sp_2, Py_3 and Al_{12} (Figure 3-3). Two analyses from altered shale have relatively high almandine contents. Green garnet from sample KL26-8 385.4m has a composition of approximately $Gr_{80}Al_{12}Py_8$ (Appendix III). Composition is not consistently correlated to lithology (Figure 3-3a) but may be related to small-scale structural setting (Figure 3-3b).

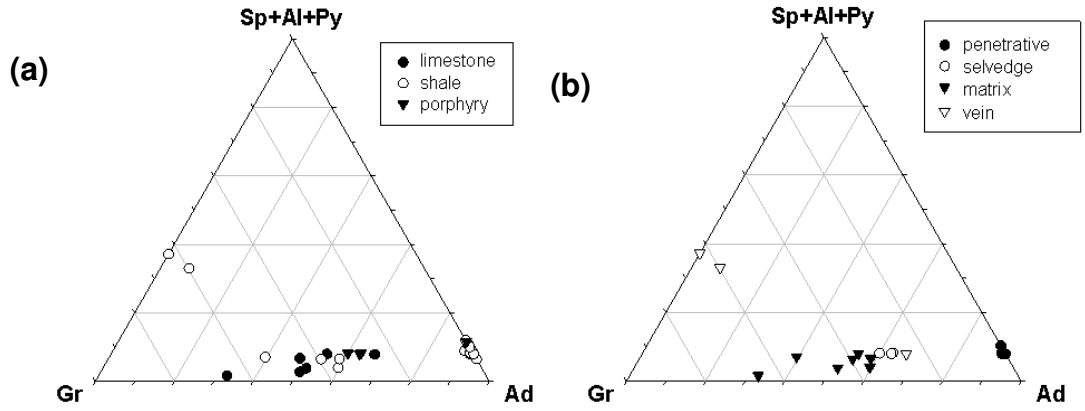

Figure 3-3 Composition of garnet

(a) Garnet analyses divided by protolith (b) Garnet analyses display some correlation with rock texture, penetrative alteration, selvedge alteration, breccia matrix replacement and vein material.

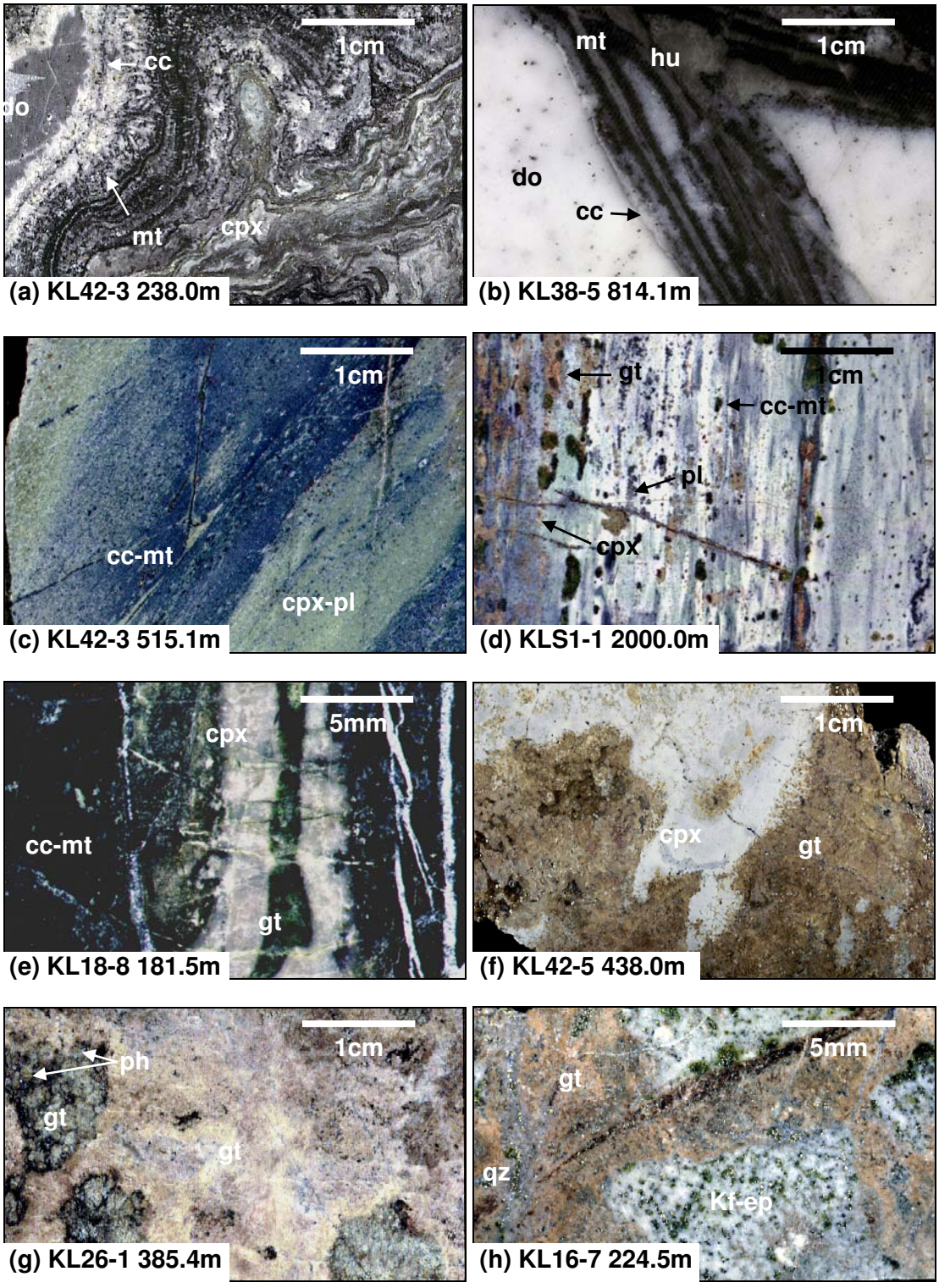

Plate 3-1 Textures and timing relationships of anhydrous Group I minerals

(a) Concentric bands of calcite, magnetite and clinopyroxene (b) Calcite, magnetite and pale brown humite selvedges (c) Clinopyroxene-plagioclase band in shale. (d) Hedenbergite-plagioclase-garnet in shale (e) Green garnet vein with white diopside selvedge (f) Penetrative white diopside alteration and green-orange coloured garnet. (g) Green garnet with green phlogopite rims in an orange-red garnet matrix. (h) Orange-red garnet selvage alteration crosscutting penetrative white K-feldspar alteration.

Humite ± forsterite ± monticellite

Humite, forsterite and rare monticellite are indistinguishable in hand specimen, though each phase has been identified via petrography and GADDS analysis (Figure 3-4). Humite is the most common; forsterite is subordinate and monticellite rare. These minerals are entirely restricted to dolomitised limestone precursors (Chapter 4). All three minerals are orange-brown (Plate 3-2a, b, c) where fresh but most of the rocks containing them are grey-black due to the presence of retrograde serpentine (Plate 3-2c, e, f). Visible forsterite veins have been identified but are uncommon (Plate 3-2b, f). Petrographic examination shows that euhedral to subhedral, equidimensional grains of humite are either evenly distributed throughout the sample or occur in locally massive concentrations. Grainsize variation of tens of microns occurs around vughs where idiomorphic grains of humite protrude inward. Humite ± forsterite is found to consistently overprint both calcite ± magnetite and clinopyroxene ± plagioclase but has no visible association with garnet. The few examples of crosscutting relationships for humite and forsterite indicate that forsterite developed after humite. Relative timing of garnet and humite-forsterite is not known as these minerals do not coexist. As garnet is closely associated with clinopyroxene, and humite overprints clinopyroxene, it is possible bur uncertain that humite-forsterite formed after garnet. Humite alteration is strongly overprinted by serpentine. Though humite is not visible in hand specimens of strongly serpentinized rocks, petrographic examination reveals that it is almost always present as isolated grains. Only nine humite samples and one clinohumite sample (7 and 9 Mg atoms respectively) were positively identified by calculation of mineral formula from microprobe compositions (Figure 3-4). Most suspected examples were established as forsterite by calculation of mineral formula from multiple analyses. Significant substitution of Fe for Mg was identified in forsterite and humite, although the amount of iron does not exceed 15wt% Total Fe. In microprobe (Appendix III) analyses of forsterite, iron is higher in vein infill than in selvage and penetrative alteration of wall rock. This broad pattern may be repeated for humite, although the number of analyses is much fewer.

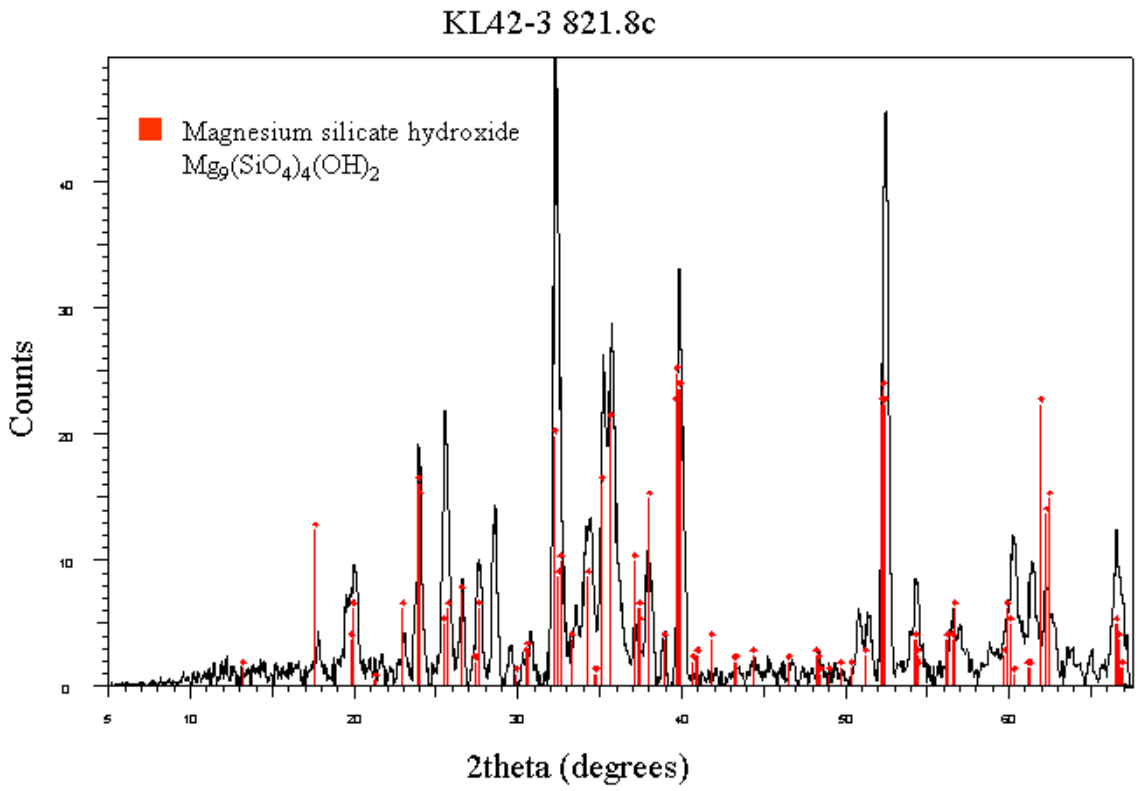

Figure 3-4 Example of GADDS X-ray diffraction identification of a humite group mineral

An overlay of output from an X-ray diffraction analysis from GADDS equipment on a type signature of peaks for a chemically identified library mineral illustrates positive identification of a humite group mineral.

Serpentine

Serpentine is consistently associated with humite ± forsterite (Plate 3-2b, c, e, f) and does not occur in clinopyroxene ± plagioclase ± garnet hornfels. Breccia fragments of humite ± forsterite found in matrices of tremolite-actinolite (next section) commonly have rims of serpentine. Serpentine is dark green to black, very soft and the grainsize varies from microscopic to millimetre-scale. Alteration is very difficult to distinguish from infill though selvage alteration and matrix alteration of fragmented rocks are the most common form at 5mm-1cm scale, rarely extending to 5cm. These fracture selvages commonly form networks in humite ± forsterite altered zones and give the appearance of 10m-scale zones of penetrative chrysotile alteration. Serpentine formed a penetrative overprint of humite ± forsterite alteration zones but is commonly overprinted by strong anhydrite alteration, producing grey-black coloured rocks in which mineral components

are difficult to recognise. Substitution of Fe into serpentine was evident in analyses but was not consistently associated with specific lithology or texture (Appendix III).

Tremolite-actinolite

Tremolite is generally restricted to clinopyroxene-altered precursors and fault zones and varies in colour from dark green, pale green, grey to almost white, although the white variety is probably the product of subsequent alteration by anhydrite and/or talc. Tremolite-actinolite forms 10cm-scale selvages on evenly spaced discrete fractures that are commonly green in penetrative clinopyroxene alteration and grey in humite-serpentine wall rocks (Plate 3-2e, f). Alteration and infill can generally be distinguished in hand sample, as infill is usually coarser-grained, though exceptions occur where grainsize is variable due to the wall rock lithology. Tremolite-actinolite commonly overprints clinopyroxene rocks but is also strongly overprinted by biotite, anhydrite and chalcopyrite ± pyrite. Replacement is gradational and interconnected patches of centimetre-scale tremolite clusters persist away from identifiable channelways. In contrast to the style of tremolite-actinolite development in skarn-altered rocks, tremolite-actinolite alteration hosted in magnetite-bearing wall rocks generally has a different appearance, being paler and forming zones of penetrative alteration up to 10m wide (see Chapter 4). The association with visible fractures is not as clear for tremolite that overprints magnetite as it is for the variety that overprints skarn. Zones of penetrative tremolite-actinolite commonly contain fragments of magnetite that form sharp boundaries with the tremolite and abundant chalcopyrite mineralisation (described below). The tremolite-actinolite grains within these zones are commonly aligned (Plate 3-2h), implying a shearing component. Microprobe analyses examples are split evenly between tremolite and actinolite (Appendix III) independent of the form of mineral development. There is some preference for infill and matrix growth to be tremolite and for selvage replacement to have actinolite. Analyses from shear-hosted samples have the lowest variability. Compositions are consistent within each sample.

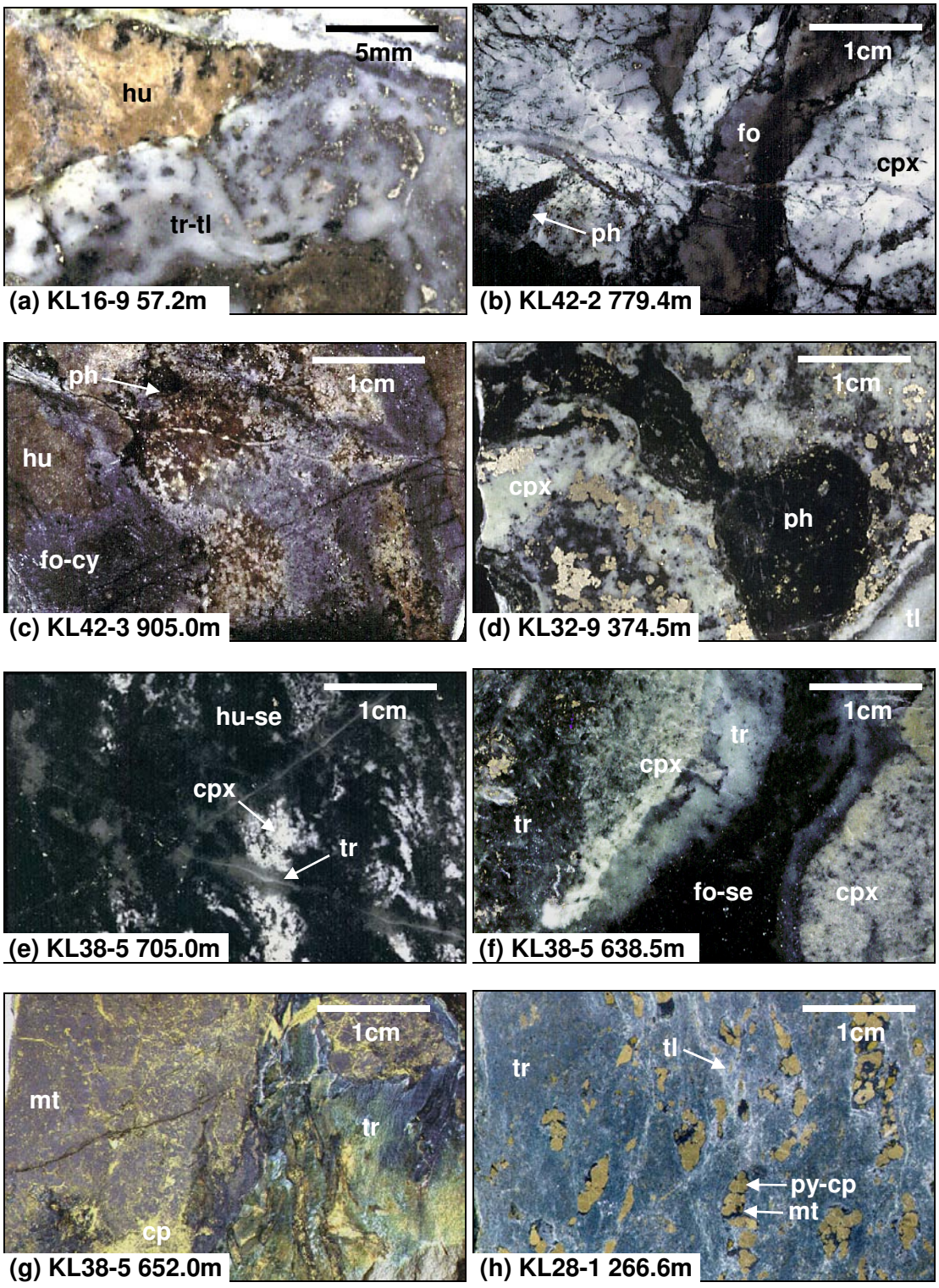

Plate 3-2 Textures and timing relationships of hydrous Group I minerals

(a) Humite fragment tremolite, talc and anhydrite matrix. (b) Forsterite vein crosscutting white diopside and overprinted by tremolite-actinolite and talc. (c) Orange-brown humite fragments in forsterite-chrysotile matrix. (d) Phlogopite alteration in clinopyroxene. (e) Clinopyroxene and humite overprinted by serpentine and tremolite (f) Serpentine and tremolite overprinting of forsterite vein in clinopyroxene wall rock. (g) Tremolite-actinolite around magnetite fragment. (h) Fibrous tremolite containing fragments of magnetite altered to pyrite-chalcopyrite.

Group II

This group is defined by potassium minerals, but also includes quartz veins which are consistently associated with K-feldspar alteration and magnetite as it appears to have a consistent temporal relationship. The minerals included in this group are:

a) K-feldspar $KAlSi_3O_8$

b) Quartz veins SiO_2

c) Mica $K(Mg,Fe)_3[Si_3AlO_{10}](OH)_2$

d) Magnetite Fe_3O_4

K-feldspar

K-feldspar occurs primarily as penetrative alteration of clinopyroxene ± plagioclase hornfels (Plate 3-3b, f, h), though examples of low intensity K-feldspar indicate association with fractures which contain sub millimetre-scale infill (Plate 3-3). Although its development is largely restricted to calcareous shale, K-feldspar is also, albeit rarely, present in rare centimetre-scale veins and selvage alteration in altered limestone (Plate 3-3f). K-feldspar is very commonly accompanied by subordinate brown biotite producing a pale brown coloured rock (Plate 3-3d, e). The relative timing of K-feldspar is well constrained as it overprints clinopyroxene-plagioclase alteration and is consistently overprinted by biotite (Plate 3-3). Where K-feldspar has been identified in limestone it is consistently found to overprint green phlogopite (Plate 3-3f). Analyses of K-feldspar from veins, selvage alteration and penetrative alteration in both shale and from an unknown precursor lithology have consistent compositions from Or_{90}-Or_{100} and are indistinguishable from each other (Figure 3-2; Appendix III).

Phlogopite-biotite

Mica occurs as both green and brown varieties, which have consistent crosscutting relationships. The green variety is referred to here as phlogopite while the brown is referred to as biotite. Phlogopite and biotite most commonly forms locally penetrative centimetre to metre-scale coarse-grained accumulations. They are locally abundant associated with millimetre to metre scale fracturing and fragmentation and it is difficult to distinguish infill and alteration as euhedral crystals are common although alteration appears to be their more dominant form. Petrographically, phlogopite is pale to transparent, with weak to moderate pleochroism the same as the visible colour, while biotite is much darker brown in colour, though pleochroism is still strong. Phlogopite is generally found in limestone and biotite in shale, however there are some exceptions, brown varieties of phlogopite found associated with humite and more rarely with clinopyroxene. The relative timing of green phlogopite is well constrained by consistent relationships where it crosscuts clinopyroxene, green garnet and humite-forsterite and is overprinted by K-feldspar. Biotite is regularly developed with K-feldspar as very pale brown fracture selvedge alteration around fracture networks in massive K-feldspar (Plate 3-3). Biotite occurs more frequently in hornfels-altered rocks but is not totally restricted to this lithology (Plate 3-3). Biotite alteration is generally fine to very fine-grained. Infill associated with K-feldspar microfractures is generally sub-millimetre scale while in quartz it is millimetre-scale.

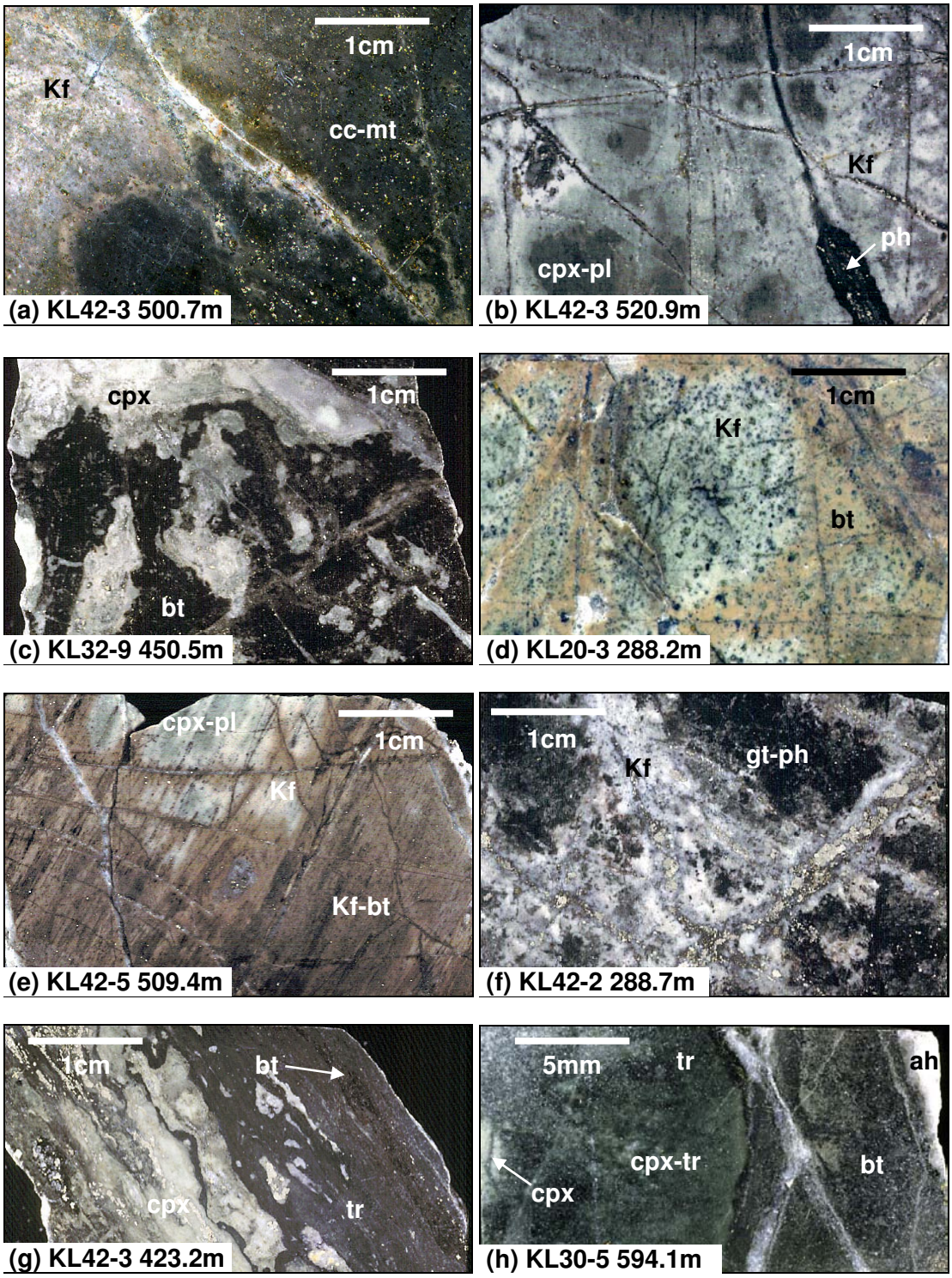

Plate 3-3 Textures and relative timing of potassic Group II minerals

(a) K-feldspar overprint of calcite-magnetite hornfels (b) Dark green clinopyroxene-plagioclase hornfels crosscut by white K-feldspar selvages (c) Biotite selvages in penetrative clinopyroxene (d) Pale biotite selvages in white K-feldspar hornfels. (e) Progressive clinopyroxene-plagioclase, K-feldspar + biotite alteration of shale. (f) Fragments of garnet and green phlogopite surrounded by selvages of K-feldspar in a limestone precursor. (g) & (h) Two examples of tremolite-actinolite crosscut by biotite along the same fracture system in limestone.

Quartz veins

A set of quartz veins that are consistent in size and spacing is associated with potassic alteration due to temporal relationships. These veins are most commonly 1cm-scale but range from 5mm-10cm and are composed of 2-5mm equant, subhedral to euhedral crystals. There is no alteration selvedge around quartz infill. Vein patterns vary from evenly spaced, sheeted arrays to multidirectional stockworks. Quartz veins are most abundant in shale and porphyry but also occur in clinopyroxene-altered limestone (Plate 3-4). Quartz veins crosscut K-feldspar altered rocks and do not contain any K-feldspar infill. An ambiguous relationship with coarse-grained biotite exists where quartz infill occurred after biotite in fractures which contrasts with biotite infill within a quartz vein (see geochronology section below). SEM investigations found microscopic titanite infill within a quartz vein sample.

Magnetite

Magnetite occurs in a variety of textural forms but most commonly as fine to medium-grained penetrative alteration. Ghost fragmental textures can be seen in samples that have been completely altered to magnetite that imply earlier rock fragmentation (Plate 3-4). Breccias with preserved precursor fragment mineralogy are found at the margins of zones of penetrative magnetite alteration (Plate 3-4). Grainsize variations can often be used to identify coarser-grained infill, but are not reliable. Other textural styles include semi-penetrative alteration in shale, isolated grains and fracture infill without associated alteration. Magnetite fracture infill is commonly irregular although regular fracture patterns were identified. Magnetite is largely confined to limestone precursors although some significant accumulations occur in fault zones and at stratigraphic contacts (see Chapter 3). While fracture-related magnetite crosscuts quartz veins and K-feldspar alteration (see Group III section), penetrative styles of magnetite are only consistently found to crosscut calc-silicate alteration. Analyses of magnetite indicate some substitution of magnesium into the lattice, up to 10 wt% MgO, but no consistent pattern to the variation could be identified (see Appendix III).

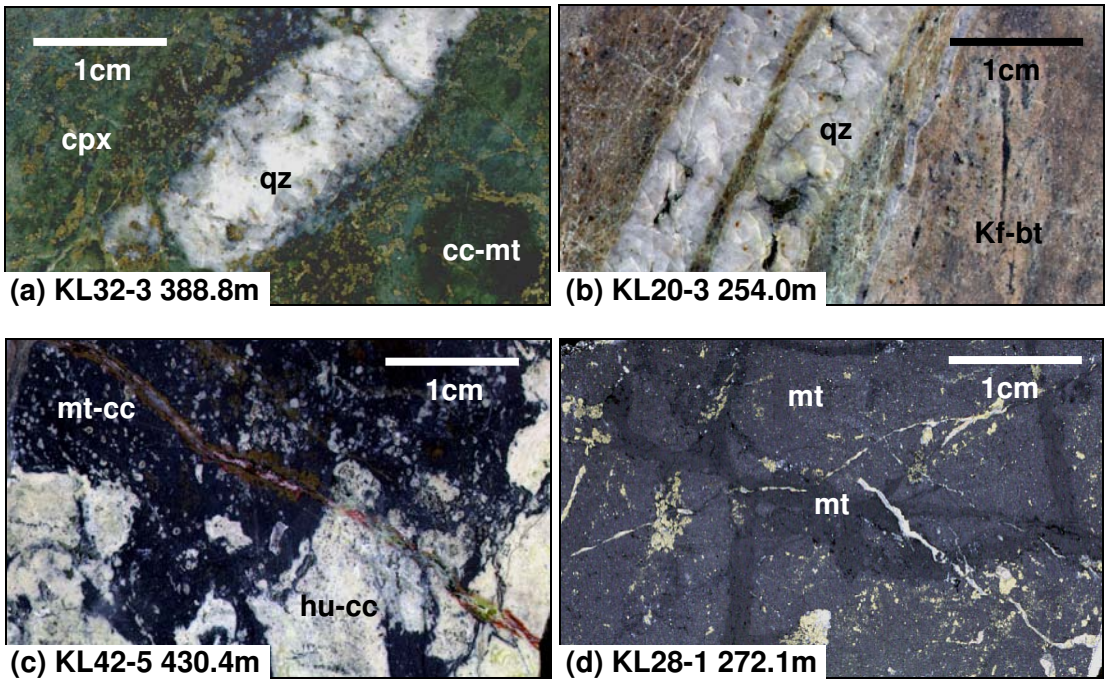

Plate 3-4 Textures and relative timing of non-potassic Group II minerals

(a) Quartz veins in penetrative clinopyroxene alteration (b) Quartz veins in K-feldspar-phlogopite hornfels. (c) Magnetite matrix surrounding calcite-altered humite fragments (d) Penetrative magnetite alteration of fragments surrounded by darker magnetite matrix.

Group III

This group is dominated by quartz (silicification) but also includes muscovite, talc and anhydrite. The distributions of minerals in this group are primarily influenced by host rock chemistry. Anhydrite is included as appears to be temporally-related. Some GADDS-XRD analyses suggested the presence of diaspore but it has not been petrographically confirmed. The minerals included in this group are:

a) Anhydrite $CaSO_4$

b) Quartz SiO_2

c) Muscovite $KAl_2[Si_3AlO_{10}](OH)_2$

d) Talc $Mg_3[Si_4O_{10}](OH)_2$

Silicification

Silicification is most commonly grey but varies from black to white. The colour variation is linked to grainsize such that white quartz is fine-medium grained while darker quartz is very fine-

grained. Black quartz is grey to white when crushed and viewed by binocular microscopy. This colour variation is reflected by infill and alteration textures (Plate 3-5c, d). Silicification generally forms 10-20cm scale selvages about individual fractures, the colour changing from white to black with distance from the fracture (Plate 3-5d). Quartz alteration occurs in all wall rocks and all previously formed alteration. Zones of penetrative quartz alteration are commonly associated with millimetre to centimetre scale, regular to irregular vughs, which occur in both clinopyroxene and K-feldspar altered rocks. The timing of quartz alteration is constrained by rare examples of quartz selvage alteration that overprint magnetite and tremolite-actinolite. The exclusion of magnetite, chrysotile and tremolite-actinolite from zones of quartz alteration where the two are juxtaposed is also used as evidence to constrain the abundant replacement quartz. Mutually exclusive muscovite and talc cannot be directly compared for timing purposes. However, the consistent associations of both of these minerals with quartz alteration, plus their similar relative timing to other minerals (talc is established as post-tremolite, while muscovite is established as post-biotite) are used as evidence that they both belong to Group III.

Anhydrite

Anhydrite is almost ubiquitous in low concentrations in rock samples from Kucing Liar but does not occur in quartz alteration. It is white to pale pink/purple in colour. It forms centimetre-scale vein and vugh infill (Plate 3-5b) devoid of associated alteration, as well as centimetre-scale fracture selvedge and metre-scale penetrative alteration. Some samples suggest that anhydrite may preferentially replace Group II quartz veins (Plate 3-5a). Veins of anhydrite in clinopyroxene-plagioclase hornfels appear spatially associated with, and similar in style to, Group II quartz veins. Anhydrite invariably crosscuts tremolite where the two are found together, and occupies the centres of tremolite channelways. Relationships between anhydrite, quartz-muscovite and chalcopyrite mineralisation (Plate 3-5g, h) indicate that anhydrite post-dates quartz ± muscovite alteration and predates Stage IV pyrite alteration and copper mineralisation. Overprinting of anhydrite by locally penetrative pyrite also supports timing relationships for anhydrite and chalcopyrite.

Muscovite – talc

These two minerals do not occur together and are believed to represent the same process in different host rocks. Talc is commonly associated with quartz alteration of clinopyroxene rock, while muscovite accompanies quartz alteration of K-feldspar rocks (Plate 3-5a, b). Both minerals are fine-grained and frequently form penetrative replacement and, rarely, veins and wispy fracture networks (Plate 3-5g, h). Muscovite and talc occur as haloes around vughs and fractures and as botryoidal infill in vughs (Plate 3-5e, f). Muscovite crystals are generally less than 50μm (see Chapter 6).

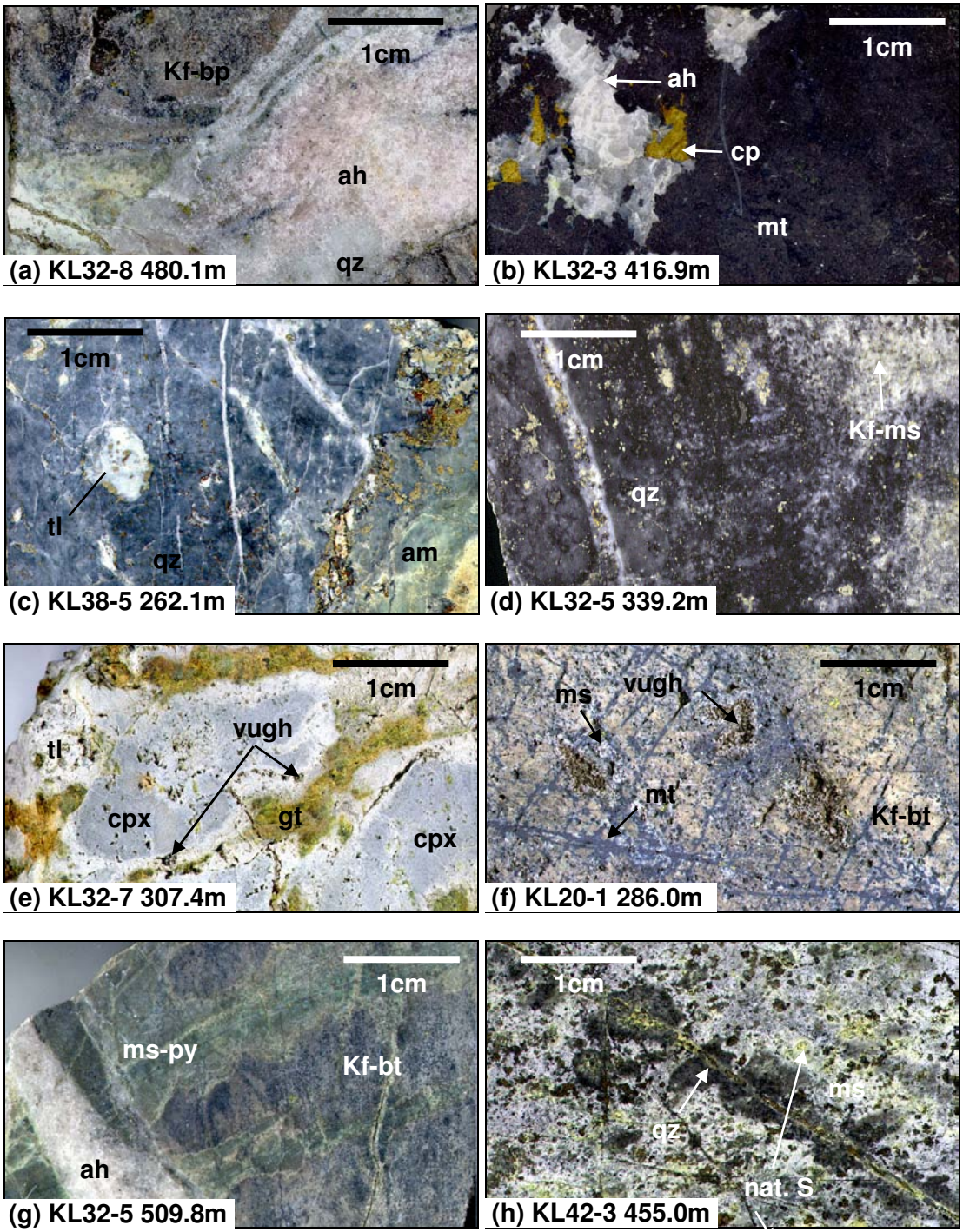

Plate 3-5 Textures and timing relationships of Group III minerals

(a) Anhydrite alteration of quartz vein (b) Anhydrite infill with chalcopyrite in magnetite. (c) Fine-grained grey quartz of clinopyroxene-tremolite altered limestone, a fragment of which is now talc. (d) Quartz + muscovite alteration of K-feldspar altered shale centred on a millimetre scale vein (left). The quartz alteration is peppered with fine pyrite and covellite spots. (e) Leach holes in clinopyroxene-garnet altered limestone associated with talc development. (f) A tension array of magnetite infill truncated by leach holes in K-feldspar-biotite altered shale lined with muscovite. (g) Anhydrite vein crosscutting muscovite-pyrite selvedge alteration in a K-feldspar-biotite altered rock. (h) Patches of muscovite + native S alteration associated with quartz selvage alteration in shale.

Group IV

Sulphide minerals dominate this group although minor amounts of fluorite, calcite, anhydrite and serpentine are included. This group includes copper mineralisation as well as locally significant accumulations of molybdenite and galena-sphalerite. The various assemblages recognised in the group are:

a) Pyrite	FeS_2
b) Pyrrhotite	Fe_{1-x} S
c) Chalcopyrite ± bornite ± digenite	$FeCuS_2$, Cu_5FeS_4, Cu_9S_5
d) Covellite ± enargite (± pyrite)	CuS, Cu_3AsS_4, FeS_2
e) Nukundamite ± covellite ± chalcocite	$Cu_{5.5}FeS_{6.5}$, CuS, Cu_2S
f) Molybdenite	MoS_2
g) Sphalerite – galena	ZnS, PbS
h) Native sulphur	S

Pyrite-pyrrhotite

There are two forms of pyrite in the Kucing Liar system. The first is very fine-grained (sub-millimetre scale) and is a muddy brass colour, while the second is consistently coarser grained (millimetre-scale) and is a brassier yellow colour (Plate 3-6). The first type is referred to as fine pyrite and the second as coarse pyrite and the two commonly occur together. Both types occur as low abundance accumulations in the form of discrete spots and as higher intensity selvages along fractures (Plate 3-6). Fractures typically contain slightly coarser grained infill. Selvages of pyrite alteration extend for tens of centimetres from fractures. Pyrite alteration is commonly penetrative and commonly constitutes 80-100% of the rock. Locally penetrative pyrite including thick accumulations of fine and coarse-grained pyrite crosscut penetrative quartz alteration. It occurs in all rock types but is most common associated with magnetite and quartz alteration (Plate 3-6). It can be difficult to distinguish coarse pyrite infill from alteration, as crystalline pyrite is a common alteration product. Lenses of massive fine and coarse pyrite crosscut penetrative magnetite and quartz alteration providing the primary criterion for its timing. Massive pyrite also crosscuts

anhydrite vein material, establishing the timing of these two minerals. Coarse pyrite appears to overprint fine pyrite, suggesting some continuous progression between the two species. Pyrrhotite occurs in similar settings to chalcopyrite and pyrite (Plate 3-6), though it is rare. Metre-scale zones of 50-100% pyrrhotite are the most common while low abundance accumulations of pyrrhotite are rare. Pyrrhotite is almost wholly restricted to major unit contacts and fault zones where it is invariably associated with locally abundant pyrite and/or chalcopyrite hosted by more extensive zones of intense magnetite alteration (Chapter 2). The relative timing of pyrite, pyrrhotite and chalcopyrite is commonly ambiguous, but where it is clear, there is a consistent sequence of pyrite → pyrrhotite → chalcopyrite (Plate 3-6c).

Chalcopyrite ± bornite ± digenite (± anhydrite)

Chalcopyrite is the dominant copper bearing sulphide in Kucing Liar and can be found in all alteration types except muscovite and talc. It has two distinct styles of development; most commonly as low intensity spots and fractures as well as 0.1-1m scale zones of locally penetrative alteration. It typically occurs as low abundances (<2%) although locally massive 1m-scale concentrations with 80-100% chalcopyrite are present (Chapter 4). There are changes of chalcopyrite form in some samples from spots to fracture infill that may represent the change from alteration to infill. Chalcopyrite commonly occurs with pyrite, though discrete occurrences of either sulphide are also common (Plate 3-6). Petrographic examination indicates that rare purple bornite and rarer blue-grey digenite both occur at the rims of chalcopyrite grains (Plate 3-6), and that digenite is consistently associated with bornite. The presence of chalcopyrite adjacent to, but not within vughs (Plate 3-5), suggests that leaching, which is directly associated with covellite mineralisation (see below), occurred after some form of chalcopyrite mineralisation. However, chalcopyrite is seen to overprint quartz alteration along with pyrite, indicating that while it predates muscovite, it postdates quartz alteration.

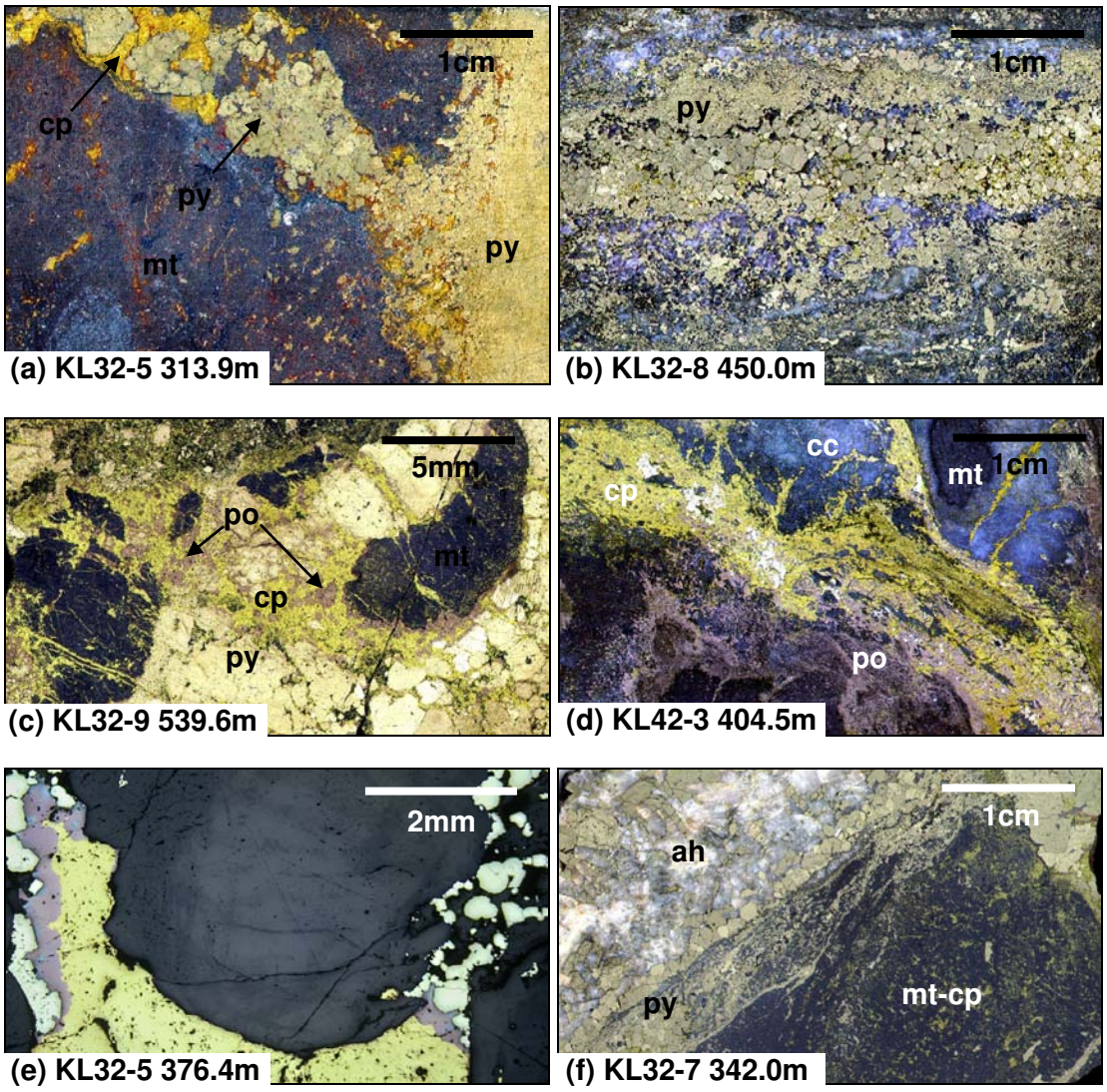

Plate 3-6 Textures and timing relationships of pyrite, pyrrhotite and chalcopyrite

(a) Pyrite alteration band including chalcopyrite in penetratively magnetite altered wall rock. Some oxidation of the sulphide minerals allows clear distinction (b) Brassy coarse pyrite selvage alteration in penetrative quartz alteration taken from the middle of a 20m zone of +80% pyrite. Darker yellow chalcopyrite is visible along the middle of the pyrite. (c) Fragments of pyrrhotite in a chalcopyrite-only matrix which crosscuts pyrite and magnetite fragments. (d) Selvage alteration and fracture infill of pyrrhotite-only and chalcopyrite-only enhance the outline the penetrative alteration of magnetite by calcite. Stringers of chalcopyrite crosscut the pyrrhotite. (e) Purple bornite and minor blue digenite alteration products at the edge of an area of chalcopyrite infill in a quartz vein. (f) Pyrite-chalcopyrite mineralisation crosscutting an anhydrite vein that is hosted by penetrative magnetite alteration. The locally penetrative pyrite is considered to form later than the chalcopyrite which is abundant in magnetite but absent in the anhydrite vein.

Covellite ± enargite ± pyrite ± native sulphur (± fluorite)

Covellite is largely restricted to specific alteration assemblages; namely, silicified and muscovite-altered rock types, although one occurrence was found in a diopside-altered rock. Fluorite is rare but occurs in association with covellite and pyrite (see Chapter 4). Covellite occurs in fractures (Plate 3-7) and vughs as infill and forms metre-scales accumulations of 40-50% by volume. Covellite grainsize is commonly sub-millimetre but millimetre-sized hexagonal crystals are not uncommon, especially within vughs. Visibly identified enargite was confirmed petrographically and is consistently associated with covellite (Plate 3-7). It is black to steel grey in hand specimen but has a pale pinkish colour when viewed in reflected light. Native sulphur occurs as infill of holes either alone or associated with pyrite-covellite. Bright yellow native sulphur is also present in distal alteration associated with quartz-dolomite-anhydrite infill of dissolved fossils (Chapter 2). Rare examples indicate that covellite ± fine pyrite overprints chalcopyrite ± brassy pyrite (Plate 3-7). However, in general, the two do not coexist.

Nukundamite, chalcocite

Nukundamite occurs as individual millimetre-scale grains and has been found in calcite (Plate 3-7) and muscovite. This assemblage is associated with muscovite alteration as well as calcite infill around pyrite breccia fragments. It is salmon pink in hand specimen and orange, exhibiting strong bireflectance when observed microscopically in reflected light. Chalcopyrite and covellite occur as laths within grains of nukundamite, while chalcocite occurs as rims at the outer edge of grains. Chalcocite was found associated with both nukundamite and covellite. Chalcocite is soft with a bluish-grey colour in hand specimen and is silver-grey microscopically.

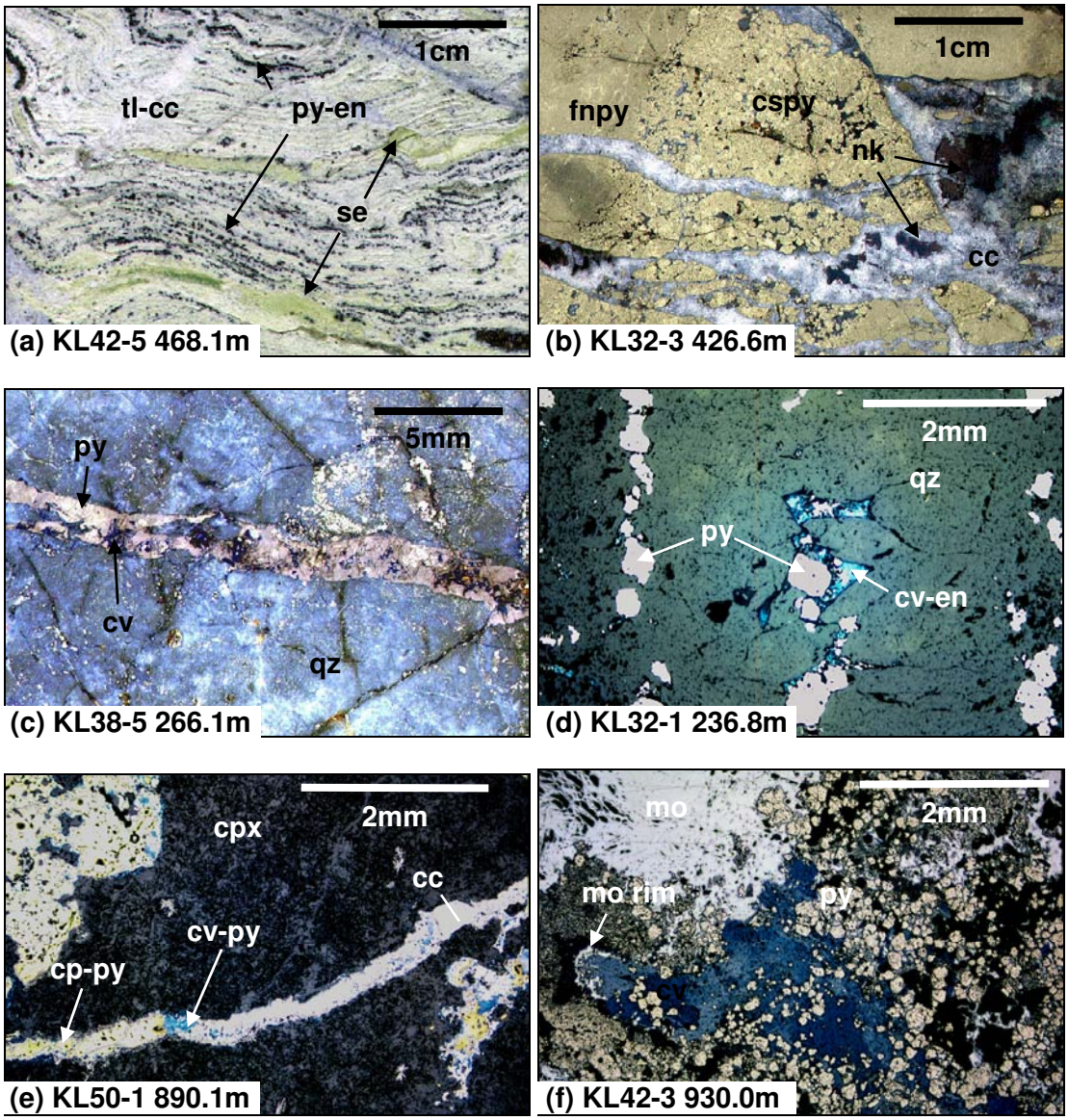

Plate 3-7 Textures and relative timing of covellite, enargite and nukundamite

(a) Bands of talc-calcite and serpentine plus thin black bands of pyrite ± enargite. (b) Fragments of fine and coarse pyrite in a calcite matrix that contains later nukundamite infill. (c) A thin vein of pyrite-covellite crosscutting penetrative quartz alteration. The sample has been finely polished to enable visibility of the blue covellite, which makes the pyrite appear a pinkish colour. (d) Covellite-enargite infill after pyrite in a quartz vein after crystalline pyrite. (e) Covellite-pyrite replacement along segments of millimetre-scale chalcopyrite-pyrite veinlets and as rims around clusters of chalcopyrite-pyrite. (f) A rim of molybdenite formed on covellite. The relationship of the molybdenite rim with the remaining solid patches of molybdenite in the view is uncertain.

Sphalerite ± galena

In addition to copper mineralisation, there are minor occurrences of lead and zinc in the form of galena and sphalerite. Sphalerite is black to brown in colour with poor crystal development. Sphalerite and galena frequently occur together as locally dense accumulations at the upper margins of the mineralised zone (Chapters 4 & 5), hosted in calcite or clinopyroxene ± garnet alteration (Plate 3-8a). Accumulations of galena-sphalerite are commonly 10cm scale, extending rarely to metre scale. They are most usually in the form of fracture infill or as replacement of matrix in fragmented rocks and polymictic breccia.

Molybdenite

Molybdenite forms radiating crystal masses and is restricted to the lowermost sections of the mineralised zone (Plate 3-8b). It is present as fracture infill and mm-scale selvage alteration most commonly hosted in quartz veins and anhydrite veins or anhydrite alteration.

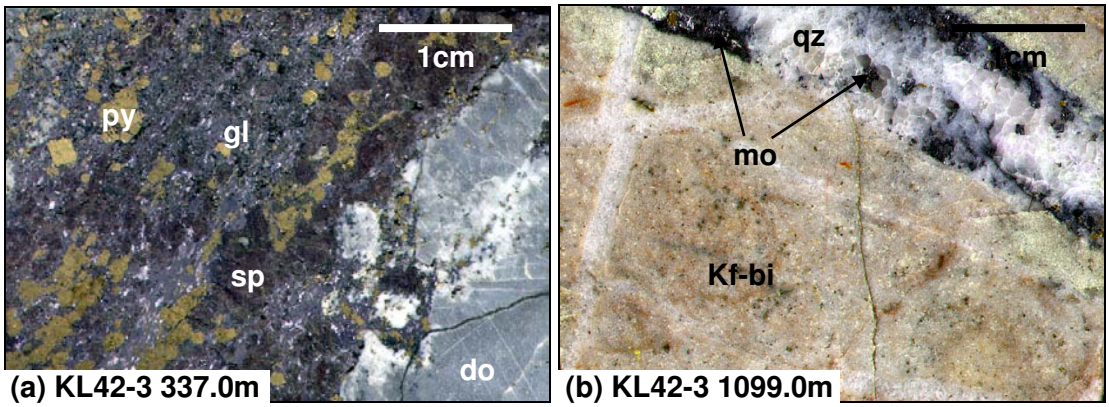

Plate 3-8 Textures and timing relationships of galena, sphalerite and molybdenite

(a) A band of galena and sphalerite fringed by calcite-altered dolomite containing fragments of pyrite. It is uncertain if the calcite rim is related to the galena-sphalerite (b) Molybdenite infill in a quartz vein hosted by K-feldspar altered Ekmai sandstone.

Intrusive rocks

Approximately 2.5% (2,266m) of drill core was positively identified as being of igneous origin, the majority of which was encountered in drill stations KL30 – KL44, adjacent to the Grasberg Igneous Complex contact zone (see Chapter 2). The igneous rocks are locally difficult to identify due to penetrative garnet alteration. A limited number of igneous rock samples were collected and their composition identified by petrography as monzodiorite and hornblende diorite. Weakly altered examples of monzodiorite are composed of 30-40% evenly distributed 5mm plagioclase phenocrysts and 5-10% phlogopite phenocrysts in a very fine-grained matrix (Plate 3-9). Both the fragment and intrusion are crosscut by biotite in the form of fracture selvage alteration whose colour changes from dark to pale brown across the sediment-intrusion contact. Monzodiorite was found in contact with pyroxene and amphibole-altered rocks while red garnet and brown biotite fracture selvage alteration was found crosscutting monzodiorite (Plate 3-9a, b). Hornblende diorite is found in only one locality at the western end of the deposit in a 15m intersection from 385-400m depth in drillhole KL42-06. The rock is grey to black and contains 10% 1-2mm hornblende and 1-2% 1-2mm brown mica phenocrysts. The hornblende phenocrysts are strongly green-brown pleochroic (Plate 3-10b) and weakly aligned. Phenocrysts are black in unaltered zones of the rock varying to green-grey where they are near bands of quartz alteration. Adjacent to quartz alteration the hornblende is replaced by talc and within the bands they are replaced by fine-grained quartz (Plate 3-10a).

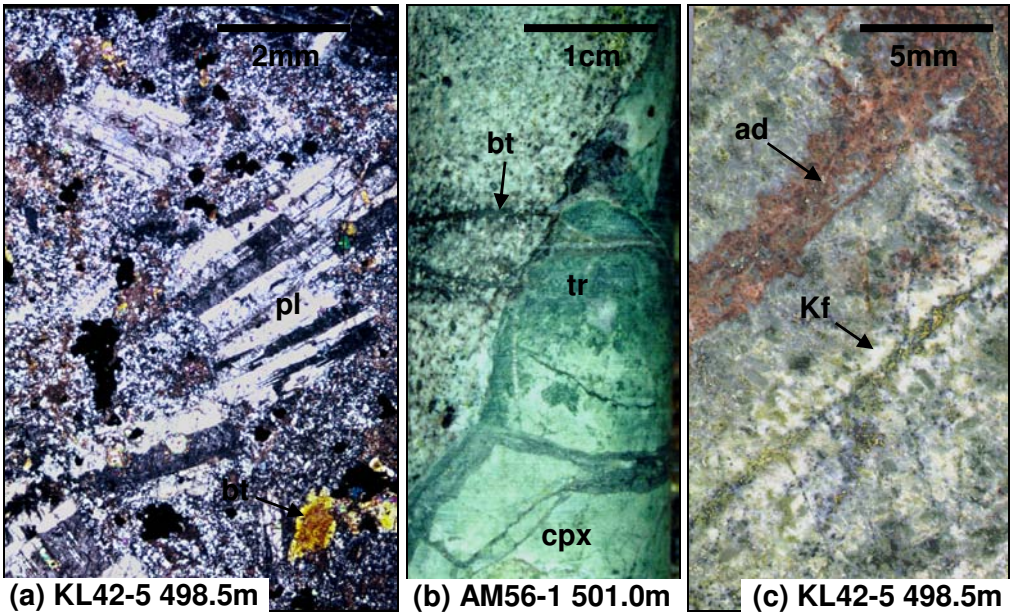

Plate 3-9 Visible and microscopic textures of common alteration effects in monzonite

(a) Photomicrograph of monzodiorite texture showing large plagioclase phenocryst in a fine-grained K-feldspar groundmass which appears to locally overprint an earlier phase of clinopyroxene alteration. (b) Clinopyroxene-tremolite skarn intruded by monzodiorite. Biotite veins crosscutting both the intrusion and the altered fragments are darker brown in the intrusion than in the skarn. The intrusion has exploited the same fracture as tremolite selvage alteration. (c) Selvage accumulations of red garnet (andradite) and K-feldspar along parallel fractures in monzodiorite.

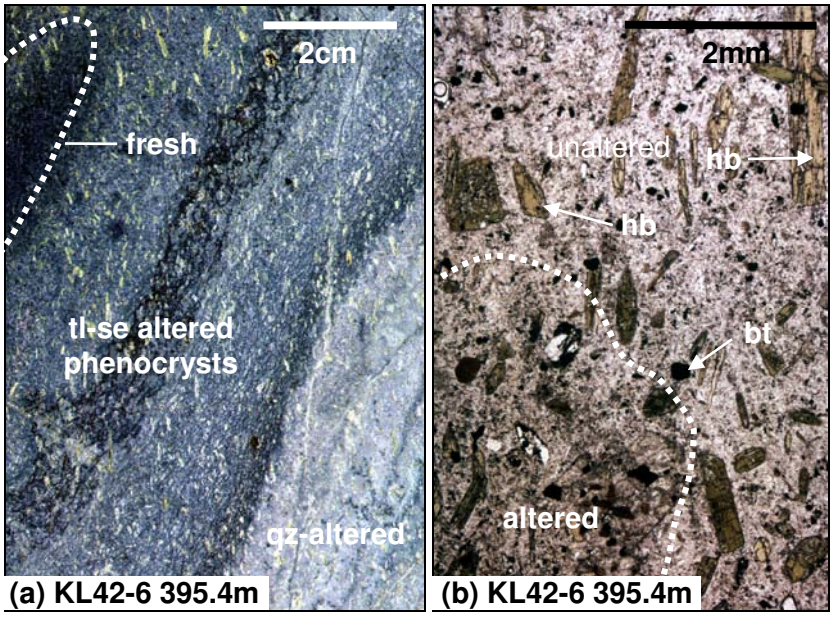

Plate 3-10 Visible and microscopic textures of diorite

(a) A band of white quartz is accompanied by a halo of talc alteration of hornblende phenocrysts in diorite A patch of unaffected rock at upper left illustrates the original texture (b) Photomicrograph of the diorite texture, to the top right the phenocrysts are unaffected by hydrothermal alteration.

3.2 INTERPRETATION OF KUCING LIAR PARAGENESIS

The following discussion begins with correlation of the key Kucing Liar hydrothermal mineral assemblages with recognised alteration assemblages that are related to porphyry-related mineralisation and places them in paragenetic context, while the second part examines the conditions of the hydrothermal system based on the key assemblages recognised in the system. There are a large number of minerals developed in Kucing Liar wall rocks that have highly variable chemistry.

Classification and inter-relationships of Kucing Liar mineral assemblages

The alteration assemblages from Kucing Liar rock samples form a complex series of relationships. The complexities are increased by lithological control of alteration where certain minerals and associations only appear in certain wall rock types (Chapter 2). Not all of the relationships are present in every sample, necessitating an approach whereby observed relationships are integrated to form a generalised sequence. There are some issues remaining where key relationships have not been observed, however, the results presented here are considered a good approximation of the paragenetic history for Kucing Liar. The hydrothermal minerals have been grouped into four broad assemblages that relate to four distinct paragenetic stages based on broad temporal relationships. Group I is characterised by a progression of calcite ± magnetite, clinopyroxene ± plagioclase, garnet, humite-forsterite. The clinopyroxene ± plagioclase has two distinct styles that are lithologically-controlled. Group I is overprinted by serpentine after humite-forsterite and tremolite-actinolite after clinopyroxene ± plagioclase, but not where it occurs as hornfels. Group II is an association of green phlogopite, K-feldspar ± biotite and magnetite. Group II magnetite is overprinted by tremolite-actinolite but tremolite-actinolite is overprinted by biotite, a convoluted relationship which will be discussed further below. Group III is an association of quartz ± muscovite ± talc and anhydrite.

Group I

A fundamental issue concerning Group I is whether or not hornfels-like alteration characterised by hedenbergite ± plagioclase alteration of calcareous shale is coeval with diopside ± garnet in limestone. Each association has different clinopyroxene compositions as well as different plagioclase abundances. Both associations are accompanied by garnet though there is a distinct difference where garnet in hornfels is consistently red, indicating high Fe-content and andradite compositions, while garnet in skarn varies from green to orange-coloured, representing a larger variation in composition from andradite to grossular. An alternative explanation to contemporaneous development of these two assemblages is that the hedenbergite ± plagioclase formed first in calcareous shale and was overprinted by K-feldspar ± biotite while adjacent limestone rocks were altered to diopside ± garnet. However, green phlogopite has overprinted clinopyroxene ± garnet and was in turn overprinted by K-feldspar, establishing that K-feldspar ± biotite is not equivalent to clinopyroxene ± garnet. Green phlogopite is also overprinted by tremolite-actinolite, and is also consistently associated with calc-silicate alteration rather than other potassic minerals, indicating it is more probably part of Group I. It is therefore maintained that the progression of Group I is calcite ± magnetite → clinopyroxene ± plagioclase → garnet → humite-forsterite → phlogopite → serpentine and finally tremolite-actinolite.

Calcite ± magnetite, diopside ± plagioclase and garnet can be described as calcic skarn due to the significant amounts of diopside-andradite within the required composition ranges, while forsterite-humite alteration is more strictly defined as magnesian skarn and retrograde alteration is the term generally used to refer to the formation of hydrous mineralogy (i.e. serpentine and tremolite-actinolite) in pre-existing skarn (Einaudi *et al.*, 1981). These could equally be referred to as anhydrous and hydrous, or prograde and retrograde skarn. Calcic clinopyroxene skarn replaces limestone and commonly consists of Fe-Ca silicates such as andradite and hedenbergite while magnesian forsterite skarn replaces dolomite and is characteristic of silica-deficient environments (Einaudi *et al.*, 1981). Copper-bearing skarn deposits in porphyry environments

tend to contain andraditic garnet (Einaudi *et al.*, 1981; Meinert, 1998). Skarn deposits typically display a successive pattern of:

(1) isochemical contact metamorphism accompanying emplacement of the magma

(2) metasomatism (skarn formation) accompanying crystallization of the magma and evolution of the ore fluid

(3) retrograde alteration accompanying final cooling of the system (Einaudi et al., 1981).

Early contact isochemical metamorphism develops light-coloured iron-poor calc-silicates, marbles and hornfels. This pattern is repeated in Kucing Liar though the presence of fracture-related selvedge alteration in the Ekmai Limestone may indicate that early hornfels was also the product of fluid infiltration rather than isochemical metamorphism. The assemblage clinopyroxene ± plagioclase is strongly lithologically-controlled as evidenced by the presence or absence of plagioclase, the texture of alteration, and the chemistry of clinopyroxene. The significantly different assemblages of diopside ± garnet and hedenbergite-plagioclase ± garnet demonstrate a strong lithological control on early stages of alteration.

The progression of alteration is visible in sandstone layers from samples taken distant from Kucing Liar (see Chapter 2), where the matrix is altered to combination of talc and amphibole, and where clinopyroxene developed at the expense of sand grains. Forsterite can develop either from metasomatism of dolomite and quartz rocks or from alteration of clinopyroxene (Einaudi et al., 1981). Retrogressive alteration involves hydration of reactions involving diopside and forsterite. Tremolite-actinolite and serpentine result from retrograde alteration of different mineral associations in the pre-existing skarn alteration. The dominant trend in retrograde alteration in skarn deposits involves the formation of hydrous silicates that are progressively depleted in calcium as the intensity of alteration increases (Einaudi *et al.*, 1981). Retrograde alteration products typically reflect the composition of the original skarn silicates; epidote, chlorite and

calcite replace grossularite, quartz, iron oxides and calcite replace andradite, biotite-hornblende-plagioclase replace almandine-rich garnet, tremolite-actinolite and eventually talc replaces diopside and serpentine replaces forsterite (Einaudi *et al.*, 1981).

Group II

The sequence of Group II minerals is difficult to interpret due to strong lithological control resulting in a lack of critical relationships. K-feldspar ± biotite is consistently found to overprint hornfels-like clinopyroxene ± plagioclase alteration, though there are localised examples of K-feldspar associated with green phlogopite in altered limestone. Group II magnetite is consistently found to crosscut clinopyroxene ± plagioclase, K-feldspar ± biotite hornfels and clinopyroxene ± garnet, humite-forsterite altered limestone. However, magnetite is also consistently overprinted by tremolite-actinolite and occasionally serpentine. Furthermore, localised biotite in limestone-altered rock consistently crosscuts tremolite-actinolite. The simplest interpretation is that a single retrograde alteration phase occurred after potassic-magnetite alteration producing the sequence clinopyroxene ± plagioclase ± garnet → K-feldspar ± biotite → magnetite → serpentine, tremolite-actinolite is equivalent to the sequence calcite ± magnetite → clinopyroxene ± garnet alteration → magnetite → serpentine, tremolite-actinolite. However, this is not consistent with biotite overprint of tremolite-actinolite. An alternative interpretation which is preferred here is that there are actually two episodes of tremolite-actinolite alteration, being before K-feldspar ± biotite and after magnetite alteration.

Alteration mineral assemblages in porphyry systems that consist of quartz, K-feldspar, biotite, anhdyrite and magnetite are named the potassic assemblage (*cf.* Lowell and Guilbert, 1970; Gustafson and Hunt, 1975; Hedenquist *et al.*, 1998; Ulrich and Heinrich, 2001a). Potassic alteration of aluminosilicate rocks is one of the characteristics of Au-bearing skarn (Meinert, 1998) and, along with an abundance of hydrothermal magnetite, distinguishes Cu-Au porphyry styles from other porphyry deposits (Sillitoe, 1979). Where potassic alteration assemblages are developed in porphyry-related skarn they generally overprint aluminous skarn hornfels rock types

(Meinert, 1998; Morrison *et al.*, 1999). One explanation for this is that the K originally present in the host rocks (see Chapter 1; Table 1-5) is liberated during skarn formation and may be incorporated into biotite ± K-feldspar alteration due to circulating fluids. A lithological control on K-feldspar alteration is consistent with observations at Kucing Liar. A second interpretation could be that the potassium has been sourced from the fluids, this is also consistent with the distribution of biotite in high flow zones (see Chapter 4), however, this does not explain the lithological control on potassic alteration. It is likely that the lithological control is a function of the aluminium content from the host rocks (Chapter 1, Table 1-5), which is incorporated into early-formed plagioclase, which in turn is altered to K-feldspar.

Although chemically distinct, magnetite is generally assigned to potassic alteration (*cf.* Lowell and Guilbert, 1970; Gustafson and Hunt, 1975; Hezarkhani and Williams-Jones, 1998) and is ubiquitous in this assemblage in Au-bearing porphyries (Sillitoe, 1997). The connection of K-feldspar ± quartz veins and magnetite are indicated at Bajo del la Alumbrera where penetrative quartz-magnetite ± K-feldspar grades laterally into K-feldspar ± biotite (Ulrich and Heinrich, 2001a). High magnetite content in skarn deposits may be a function of the dolomitic wall rocks, in which Fe-rich calc-silicates are not stable (Einaudi *et al.*, 1981). Elevated magnetite may also indicate the highly oxidized state for the hydrothermal fluids (e.g. Sillitoe, 1997), while the appearance of titanite in quartz veins further constrains the composition of potassic-forming hydrothermal fluids to the boundary between relatively reducing and oxidising conditions described by the assemblage quartz + titanite + magnetite (Xirochakis *et al.*, 2001). Both quartz and magnetite must be derived from the hydrothermal fluids as no major sources of Fe and Si are locally available. The quartz in sandstone may locally provide a source of silica for the development of clinopyroxene and garnet (Chapter 3), though no large-scale dissolution of the quartz sandstone units is evident.

Group III

The Group III assemblage is characterised by quartz alteration accompanied by muscovite and talc and anhydrite alteration, which individually overprint potassic and calc-silicate alteration. Sulphide mineralisation typified by pyrite, chalcopyrite ± bornite, covellite ± enargite and galena-sphalerite has been placed within this group, as it appears to be part of the broader assemblage. This lack of any other significant overprint of quartz alteration (other than sulphide) indicates that this mineral assemblage has overprinted all silicate phases. Local relationships indicate that silicification overprints skarn and potassic alteration, though pyrite is more common in magnetite. Timing relationships between anhydrite and quartz are not commonly observed though in some cases show that anhydrite overprinted quartz and muscovite alteration. Anhydrite is consistently overprinted by pyrite. Group III also includes covellite ± enargite ± pyrite mineralisation which is most prevalent as infill in vuggy quartz alteration. Less abundant mineralisation includes bornite, digenite accompanying chalcopyrite and nukundamite and chalcocite accompanying covellite. A rare assemblage consisting of nukundamite ± chalcocite is also recognised associated with alteration dominated by muscovite rather than quartz. Locally penetrative galena-sphalerite pyrite developed at the margins of the main metasomatic zone. Some molybdenite is also recognised as forming after anhydrite and overprinting covellite ± pyrite ± enargite.

The assemblage quartz ± muscovite ± pyrite is characteristic of phyllic alteration of porphyry deposits and, in conjunction with locally massive pyrite, also characterizes the “silica-pyrite” alteration found in skarn systems (Einaudi *et al.*, 1981). Silica-pyrite may replace skarn, but also replaces limestone as massive irregular bodies, mantos, or steep structurally controlled breccia pipes (Einaudi *et al.*, 1981). This is consistent with Kucing Liar, where both quartz alteration and massive pyrite are found in both skarn and unaltered limestone. A direct correlation exists between sericitic (phyllic) alteration of the pluton and the formation of silica-pyrite in adjacent skarn (Einaudi *et al.*, 1981). Covellite ± pyrite ± enargite mineralisation is one of the characteristic assemblages that define high sulphidation mineralisation, which is commonly pyrite-rich and typified by enargite, luzonite, digenite, chalcocite, covellite and nukundamite (*e.g.*

Sillitoe, 1999; Inan and Einaudi, 2002). Although high sulphidation mineralisation is generally confined to advanced argillic alteration zones typified by quartz, alunite, kaolinite or diapsore (*cf.* Hedenquist *et al.*, 1998), at some localities it extends into the sericitic (phyllic) zone, commonly zoning from advanced argillic to phyllic, which subsequently grades downwards into potassic alteration (Sillitoe, 1999). This is the case at Kucing Liar where high sulphidation mineralisation is generally formed in quartz-pyrite-muscovite alteration, though its independence from phyllic (silica-pyrite) alteration is recorded in the occurrence, albeit rare, of covellite in calc-silicate skarn. A significant problem with the Kucing Liar paragenesis is the relationship between chalcopyrite and covellite mineralisation. The sequence of development is not rigidly constrained, as the timing of sulphide minerals is commonly questionable, due to ambiguous sulphide growth textures and almost complete absence of rocks containing both of the main Cu-bearing phases. Both Cu-bearing sulphides are associated with pyrite, though chalcopyrite tends to be developed in association with coarse, brassy pyrite rather than fine pyrite.

Petrologically defined conditions of the Kucing Liar hydrothermal system

The early stages of the paragenesis indicate moderate to high temperatures and near neutral pH, while the later stages demonstrate a significant lowering of temperatures and pH conditions. Solutions associated with quartz monzonite will be nearly neutral and enriched in iron relative to magnesium (*cf*. Einaudi et al., 1981).

Studies of numerous skarn deposits around the world indicate temperatures of formation for prograde skarn (Chapter 2) between 400ºC and 650º and that there is a relationship between temperature and pressure where lower pressures lower the temperature limits of skarn formation (Einaudi et al., 1981). Skarn minerals (monticellite) from the DOM deposit have high temperature (~700°C) and high salinity fluid inclusions (Meinert et al., 1997), while Big Gossan and EESS skarn minerals, preserve much lower temperature fluid inclusions (300-500°C) of more moderate salinity (Meinert et al., 1997).

Potassium silicate alteration in porphyry-related hydrothermal systems is generally believed to form during initial cooling of magmatic brines from 600º to 400º (*cf*. Einaudi *et al*., 1981; Sillitoe, 1997; Hedenquist *et al*., 1998). The appearance of titanite in the quartz veins may have a bearing on the composition of hydrothermal fluid. The assemblage titanite + magnetite + quartz is generally thought to mark the boundary between relatively reducing and oxidising conditions and likely more common in relatively Fe-rich bulk compositions and for decreasing temperature and pressure conditions (Xirochakis *et al.*, 2001). The elevated magnetite reflects the highly oxidized state of the magma from which gold-transporting fluids were derived (Sillitoe, 1997).

Extensive late replacement of prograde skarn by retrograde skarn and silica-pyrite presumably reflects the presence of a long-lived, sulphur rich hydrothermal system operating in a highly fractured, hence permeable, environment (Einaudi et al., 1981). A decrease in temperature, oxidation by groundwater influx and low pressure boiling can all contribute to the generation of hydrothermal fluids that are out of equilibrium with plutons and skarns (Einaudi *et al.*, 1981; Meinert *et al.*, 2003), which leads to the development of retrograde alteration. Temperatures for retrograde alteration generally range from 450º to 300ºC (Einaudi *et al.*, 1981). More specifically, serpentinisation of forsterite-bearing magnesian skarn (Chapter 2) in low-pressure environments implies temperatures less than 420ºC (Einaudi *et al.*, 1981). The more pervasive retrograde replacement of magnesian skarn compared to calcic skarn reflects the instability of forsterite in water-rich fluids in temperatures below 400ºC (Einaudi *et al.*, 1981).

The presence of muscovite and quartz-covellite indicate mildly acidic conditions and moderate temperatures. Sericite-stable alteration assemblages are associated with cooler, less saline water (Hedenquist et al., 1998). However, the absence of kaolinite or alunite may indicate that highly acidic conditions were not achieved. The contrasting mineralisation assemblages recognised in Kucing Liar indicates different fluid conditions as covellite is related to slightly acidic conditions and high sulphidation stages while chalcopyrite deposits under more neutral acidity and intermediate sulphidation states (e.g. Einaudi et al., 2005).